

Pyridostigmine but not 3,4-diaminopyridine exacerbates ACh receptor loss and myasthenia induced in mice by muscle-specific kinase autoantibody

Marco Morsch¹, Stephen W. Reddel², Nazanin Ghazanfari¹, Klaus V. Toyka³ and William D. Phillips¹

¹Physiology and Bosch Institute, University of Sydney, Sydney, New South Wales 2006, Australia

²Department of Molecular Medicine, Concord Hospital, Concord, New South Wales 2139, Australia

³Department of Neurology, University of Würzburg, Josef-Schneider-Straße 11, 97080 Würzburg, Germany

Key points

- A mouse model of anti-muscle-specific kinase (MuSK) myasthenia gravis was used to study the effect of pyridostigmine (a cholinesterase inhibitor drug commonly used in myasthenia) on the disease process at the neuromuscular junction.
- In mice receiving injections of anti-MuSK-positive patient IgG, pyridostigmine treatment for 7–9 days did not prevent myasthenia, and even precipitated weakness.
- Pyridostigmine treatment potentiated the anti-MuSK-induced reductions in postsynaptic acetylcholine receptor density and endplate potential (EPP) amplitude.
- 3,4-Diaminopyridine, a drug that increases the number of quanta released (rather than the duration of each quantal response), elevated EPP amplitude without exacerbating the anti-MuSK-induced loss of acetylcholine receptors.
- The results suggest that cholinergic- and MuSK-mediated signalling may converge postsynaptically to regulate the mature acetylcholine receptor scaffold.

Abstract In myasthenia gravis, the neuromuscular junction is impaired by the antibody-mediated loss of postsynaptic acetylcholine receptors (AChRs). Muscle weakness can be improved upon treatment with pyridostigmine, a cholinesterase inhibitor, or with 3,4-diaminopyridine, which increases the release of ACh quanta. The clinical efficacy of pyridostigmine is in doubt for certain forms of myasthenia. Here we formally examined the effects of these compounds in the antibody-induced mouse model of anti-muscle-specific kinase (MuSK) myasthenia gravis. Mice received 14 daily injections of IgG from patients with anti-MuSK myasthenia gravis. This caused reductions in postsynaptic AChR densities and in endplate potential amplitudes. Systemic delivery of pyridostigmine at therapeutically relevant levels from days 7 to 14 exacerbated the anti-MuSK-induced structural alterations and functional impairment at motor endplates in the diaphragm muscle. No such effect of pyridostigmine was found in mice receiving control human IgG. Mice receiving smaller amounts of MuSK autoantibodies did not display overt weakness, but 9 days of pyridostigmine treatment precipitated generalised muscle weakness. In contrast, one week of treatment with 3,4-diaminopyridine enhanced neuromuscular transmission in the diaphragm muscle. Both pyridostigmine and 3,4-diaminopyridine increase ACh in the synaptic cleft yet only pyridostigmine potentiated the anti-MuSK-induced decline in endplate ACh

receptor density. These results thus suggest that ongoing pyridostigmine treatment potentiates anti-MuSK-induced AChR loss by prolonging the activity of ACh in the synaptic cleft.

(Received 16 January 2013; accepted after revision 20 February 2013; first published online 25 February 2013)

Corresponding author W. D. Phillips: School of Medical Sciences (Physiology) and Bosch Institute, Anderson Stuart Bldg (F13), University of Sydney, NSW 2006, Australia. Email: william.phillips@sydney.edu.au

Abbreviations: 3,4-DAP, 3,4-diaminopyridine; ACh, acetylcholine; AChE, acetylcholinesterase; AChR, acetylcholine receptor; AM, patient anti-MuSK IgG; CMAP, compound muscle action potential; EPP, endplate potential; Lrp4, lipoprotein receptor-related protein 4; mEPP, miniature endplate potential; MG, myasthenia gravis; MGFA, Myasthenia Gravis Foundation of America; MuSK, muscle-specific kinase; NMJ, neuromuscular junction; TA, tibialis anterior (muscle).

Introduction

In autoimmune myasthenia gravis (MG) muscle weakness and fatigue is caused by autoantibodies that modify the structure and function of the neuromuscular junction (NMJ). Most cases of MG have IgG autoantibodies against binding sites on the acetylcholine receptor (AChR). They cause synaptic failure by accelerating AChR degradation and by activating complement (Engel *et al.* 1977; Toyka *et al.* 1977; Drachman *et al.* 1978). Depending on latitude, approximately 5–10% of MG patients possess autoantibodies against muscle-specific kinase (MuSK) instead of the AChR autoantibodies (Hoch *et al.* 2001; Vincent *et al.* 2003; Gomez *et al.* 2010). The pathogenic effects of anti-MuSK autoantibodies appear to arise largely from the IgG4 subclass (Hoch *et al.* 2001; Klooster *et al.* 2012; Mori *et al.* 2012b). Together with the low-density lipoprotein receptor-related protein 4 (Lrp4), MuSK forms the core of a receptor–tyrosine kinase complex that mediates nerve–muscle signalling and helps to coordinate and stabilise the AChR cluster at the developing NMJ (Glass *et al.* 1996; Kim *et al.* 2008; Zhang *et al.* 2008; Wu *et al.* 2012; Yumoto *et al.* 2012).

The endplate damage caused by MuSK autoantibodies may not depend upon the activation of complement (Klooster *et al.* 2012; Mori *et al.* 2012b). Instead MuSK autoantibodies seem to somehow interfere with a physiological role of MuSK in maintaining the mature NMJ (Klooster *et al.* 2012; Mori *et al.* 2012c; Morsch *et al.* 2012; Viegas *et al.* 2012). In animal models, anti-MuSK caused NMJ impairment and myasthenic weakness due to loss of postsynaptic AChRs and nerve terminals (Jha *et al.* 2006; Shigemoto *et al.* 2006; Cole *et al.* 2008, 2010; Punga *et al.* 2011; Richman *et al.* 2011; Morsch *et al.* 2012). These changes are reminiscent of the effects of postnatal knock-down of MuSK gene expression (Kong *et al.* 2004; Hesser *et al.* 2006).

During development, endplate AChR density depends upon competing signals that regulate assembly and disassembly of AChR. MuSK can be activated by neural agrin, a proteoglycan released by the presynaptic nerve terminal. Multiple signalling complexes downstream of MuSK contribute to the assembly and stabilisation

of AChR clusters (Wu *et al.* 2010; Ghazanfari *et al.* 2011). The MuSK–Lrp4 complex may also play a structural role in helping to coordinate components of the developing NMJ (Bromann *et al.* 2004; Wu *et al.* 2012; Yumoto *et al.* 2012). In contrast, AChR channel activation may drive a pathway involving subsynaptic inositol-1,4,5-trisphosphate receptors, calpain and cyclin-dependent kinase 5 that can dismantle AChR clusters (Lin *et al.* 2005; Misgeld *et al.* 2005; Chen *et al.* 2007; Zhu *et al.* 2011). According to this view, at the developing NMJ MuSK-mediated signalling promotes the growth of AChR clusters while acetylcholine (ACh)-induced subsynaptic calcium fluxes may help to prune AChR clusters (Ono, 2008). These findings from the embryonic NMJ prompted us to investigate the possible influence of drugs that enhance synaptic ACh in a mouse model of anti-MuSK MG.

Pyridostigmine is the recommended first line of symptomatic treatments for patients with MG (Drachman, 1994; Richman & Agius, 2003; Skeie *et al.* 2010). Pyridostigmine inhibits synaptic cleft acetylcholinesterase (AChE), thereby prolonging the action of ACh upon postsynaptic AChRs. Cholinesterase inhibitors like pyridostigmine are generally well tolerated and can offer remarkable short-term benefits to MG patients (Roche, 1935). Clinical reports in anti-MuSK MG indicate variable efficacy for pyridostigmine and sometimes deterioration (Evoli *et al.* 2003; Sanders *et al.* 2003; Hatanaka *et al.* 2005). Moreover, recent electromyographic studies have reported signs of neuromuscular hypersensitivity when mice previously immunised with MuSK were acutely exposed to acetylcholinesterase inhibitors (Chroni & Punga, 2012; Mori *et al.* 2012b). Some early studies reported evidence of excitotoxic-like structural changes in otherwise healthy NMJs following long-term or high-dose exposure to AChE inhibitors (Chang *et al.* 1973; Engel *et al.* 1973; Hudson *et al.* 1985, 1986; Drake-Baumann & Seil, 1999).

In clinical practice, pyridostigmine is used chronically, but its efficacy often wanes over weeks or months (Drachman, 1994). We postulated that the immediate benefits of pyridostigmine might be overtaken by

the longer-term harmful effects of ACh persistence at the NMJ. Specifically we hypothesised that this would be most evident in anti-MuSK MG where the MuSK signalling pathway is perturbed. Lambert–Eaton myasthenic syndrome and certain congenital myasthenias are often treated with 3,4-diaminopyridine (3,4-DAP) (Banwell *et al.* 2004). 3,4-DAP acts on the presynaptic nerve terminal to increase the number of quanta of ACh released per nerve impulse (Thomsen & Wilson, 1983; Wu *et al.* 2009; Mori *et al.* 2012a). Thus, pyridostigmine prolongs the activity of ACh in the synaptic cleft, while 3,4-DAP increases the number of quanta released presynaptically. The effects of on-going treatment of anti-MuSK MG with either pyridostigmine or 3,4-DAP have not been tested in controlled experiments in animals or in patients. Here we provide the first evidence that pyridostigmine (acting postsynaptically) exacerbates anti-MuSK-induced loss of endplate AChRs while 3,4-DAP (acting presynaptically) can produce a modest improvement in neuromuscular transmission without exacerbating structural impairment at the NMJ.

Methods

Ethical approval

The article by G. B. Drummond (Drummond, 2009) was read carefully to be sure that our experiments complied with the policies and regulations regarding animal experimentation and other ethical matters. A total of 69 mice were used in this study. All mouse experiments described in this paper were conducted with the approval of The University of Sydney Animal Ethics Committee in compliance with the NSW Animal Research Act 1985 and the Australian Code of Practice for the Care and Use of Animals for Scientific Purposes 7th Edition NHMRC 2004. Patient informed, written consent was obtained in accordance with the *Declaration of Helsinki*. The project was approved by the Human Research Ethics Committee of the Sydney South West Area Health Service.

Injection of patient IgG

Six-week-old female C57Bl6J mice (Animal Resources Centre, Murdoch, WA, Australia) were group-housed and were fed *ad libitum* on rat and mouse chow (YSF brand). They received daily intraperitoneal (i.p.) injections of human IgG as previously described (Cole *et al.* 2008, 2010). Batches of anti-MuSK-positive patient IgG and control human IgG (seronegative for both MuSK and AChR) were collected when patients were suffering myasthenia gravis weakness grades 2 to 4B (Myasthenia Gravis Foundation of America (MGFA) score; Supplemental Methods and Supplemental Table S1, available online only).

Assessment of weakness and electromyography

Grade 1 weakness refers to a mouse that lay prone for ≥ 1 min after a brief exercise regime as described (Stacy *et al.* 2002). Grade 2 signifies the same behaviour prior to any exercise. Mice had to be killed (pentobarbitone 30 mg i.p.) when they reached grade 2 for ethical reasons. Repetitive stimulation of the phrenic nerve and compound muscle action potential (CMAP) recordings from the diaphragm were performed *in vitro* as previously described (Morsch *et al.* 2012). Briefly, the hemidiaphragm was isolated and pinned out in oxygenated Ringer solution. The recording electrode was placed on the surface of the diaphragm while the reference electrode was immersed in the bath solution.

Drug treatments

Pyridostigmine was delivered to mice systemically and continuously for 7–9 days via an Alzet minipump (model 1007D or 1002; Durect Corporation, Cupertino, CA, USA). Mice were anaesthetised with 1–3% iso-flurane/oxygen by inhalation and the depth of anaesthesia was monitored based upon the foot withdrawal reflex and respiratory rate. The pump was implanted beneath the skin of the mid back. Pumps were loaded with 23.6 mg ml⁻¹ pyridostigmine bromide (Sigma, St Louis, MO, USA), diluted in a buffer identical with the vehicle used for control experiments containing (in mg ml⁻¹): citric acid monohydrate 1.3, sodium citrate dehydrate 4.1, methyl paraben 0.5, propyl paraben 0.05 and NaCl 7.4 in sterile water (pH 5.1). According to the manufacturer's specifications the delivery rate was 11.8 μ g h⁻¹, providing an effective dose of ~ 16 mg kg⁻¹ day⁻¹. Buprenorphine (0.03 mg kg⁻¹ s.c.) (Reckitt Benckiser, Australia) was given for analgesia at the installation of the pump and 24 h later. The effect of different doses of pyridostigmine upon whole-blood AChE activity was determined 7 days after implantation of the minipump as described (Haigh *et al.* 2008) with minor modifications (Supplemental Fig. S1). Mice were killed with pentobarbitone (30 mg i.p.; Cenvet Australia). At the dose employed, the mice did not display evidence of cholinergic intoxication such as nasal secretions or muscle fasciculations. 3,4-DAP (Sigma), which increases ACh quanta release, was used under identical experimental conditions. Based upon the acute dosage described previously (Mori *et al.* 2012a), 3,4-DAP was diluted in vehicle and applied to yield an effective dose of 8 mg kg⁻¹ day⁻¹.

Confocal microscopy and NMJ morphometry

Cryosections were stained for nerve terminals with anti-synaptophysin and for postsynaptic AChRs with Alexa555- α -bungarotoxin. Sections were imaged (Zeiss

LSM510 Meta confocal microscope) and endplate morphometry was performed as described previously (Gervásio & Phillips, 2005; Morsch *et al.* 2012). Endplate AChE was labelled with fasciculin 2 (Latoxan, France) conjugated to Alexa647 (Krejci *et al.* 2006) as described in the Supplemental Methods. For comparison of AChR staining intensities, sections were examined in the same imaging session using identical settings. The scoring in Fig. 9 was by a blinded observer (N.G.).

Endplate potential recordings

Spontaneous miniature endplate potential (mEPP) and evoked endplate potential (EPP) recordings were made from phrenic nerve–hemidiaphragm preparations at physiological calcium levels (1 mM MgCl₂, 2 mM CaCl₂) as previously described (Morsch *et al.* 2012). Contraction was blocked using the muscle sodium channel blocker, μ -conotoxin GIIIB (1 μ M μ CTX, Peptide Institute, Japan). EPP and mEPP recordings were performed 30–60 min after the diaphragm was placed in the bath solution to allow for a wash-out of the systemically applied drugs. Spontaneous mEPP amplitudes were recorded for 1–3 min and were normalised to a resting potential of -80 mV. A train of 40 stimuli (1 s⁻¹) was used for EPP analyses. EPP amplitudes were normalised to -80 mV and then corrected for non-linear summation (Wood & Slater, 1997). Quantal content was calculated by dividing the normalised and corrected EPP amplitudes by the normalised mEPP amplitude for each muscle fibre.

Statistics

Comparison of more than two groups was by one-way ANOVA with Bonferroni's correction for multiple comparisons. Comparison of two groups was by unpaired, two-tailed Student's *t* test after checking for symmetrical distribution and similar variance of the groups under study. Statistical significance was taken as $P \leq 0.05$. Data are presented graphically in figures as mean \pm SEM. Scatter plots were fitted by linear regression.

Results

Pyridostigmine can accelerate anti-MuSK-induced weakness

In a first series of experiments mice were injected with IgG from severely affected anti-MuSK patients (AM5 or AM4.4; both MGFA 4B at plasmapheresis; Supplemental Table S1). The mice lost weight and became weak after 11–14 days, consistent with previous experiments (Cole *et al.* 2008). Weakness progressed from grade 1 (active at rest but weakness after exercise) to reach grade 2 (weakness even before exercise) at day 14. Another set

of mice was treated additionally with pyridostigmine bromide (~ 16 mg kg⁻¹ day⁻¹) for the last 7 days of the IgG injection series via an osmotic minipump implanted subcutaneously. These mice also lost weight and became weak (Fig. 1A and B). In naive mice delivery of pyridostigmine at this rate inhibited whole-blood cholinesterase activity by $39 \pm 4\%$ without any signs of toxicity (Supplemental Fig. S1). Mice injected with control human IgG did not lose weight nor did they display muscle weakness, whether treated with pyridostigmine or vehicle (Fig. 1A). Thus, in the severely affected mice pyridostigmine treatment starting from day 7 neither prevented nor delayed the progression of weakness.

We next investigated the impact of pyridostigmine in mice that were less severely affected by anti-MuSK antibodies. Mice injected with AM4.2, a batch of IgG collected when patient 4 was suffering only mild symptoms (MGFA 2B), showed neither weight loss nor muscle weakness over the 14 day injection series, whether

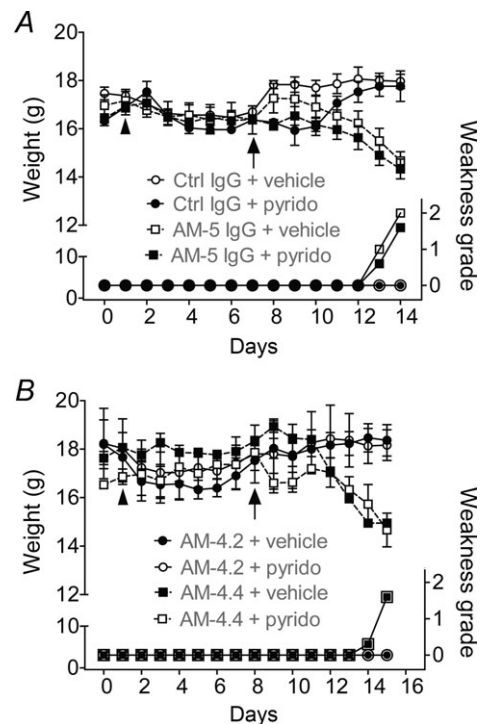


Figure 1. Effects of anti-MuSK IgG injections and pyridostigmine treatment on body weight and muscle weakness

A, average body weights and weakness grades of mice receiving daily injections of IgG from anti-MuSK patient AM5 or control human IgG (Ctrl). The arrow-head indicates a single injection of cyclophosphamide given to suppress an immune response to the human IgG. A minipump delivering either pyridostigmine or vehicle was implanted subcutaneously on day 7 (arrow). Average weakness grade is indicated by the symbols in the lower part of the panel and by the right ordinate. B, body weights and weakness grades for mice receiving IgG from patient AM4 (batch 4.2 or 4.4) and treated with pyridostigmine or vehicle as above. Error bars represent the mean \pm SEM for $n = 3$ mice in each treatment group.

treated with pyridostigmine or vehicle (Fig. 1*B*). However, when the treatment period was extended pyridostigmine exacerbated myasthenia gravis. In a follow-up experiment mice received daily injections of AM4.5 IgG (25 mg day^{-1}) for 17 days. Mice treated with vehicle did not display weakness, even after 17 days (Fig. 2, open circles). However, those treated with pyridostigmine lost weight and developed severe muscle weakness from days 15 to 17 (Fig. 2, filled squares). Hence, rather than preventing weakness, pyridostigmine was capable of precipitating weakness.

Pyridostigmine can potentiate anti-MuSK-induced changes in endplate AChRs

On immunohistochemistry, motor endplates of control and naive mice typically displayed a large pretzel-shaped AChR plaque, covered by an anti-synaptophysin-stained nerve terminal (Fig. 3*A–C*). In both the tibialis anterior (TA) and diaphragm muscles daily injections of anti-MuSK IgG (AM5 or AM4.4) for 15 days caused significant reductions in the staining intensity and/or aggregate area of postsynaptic AChR clusters (Fig. 4, grey bars). Injection of AM4.2 significantly reduced AChR cluster intensity and area in the diaphragm but not in the TA muscle. Thus all three batches of anti-MuSK patient IgG caused significant dismantling of postsynaptic AChR clusters. Treatment of the anti-MuSK-injected mice with pyridostigmine from day 8 to 15 appeared to exacerbate

the loss of AChRs from endplates in the diaphragm muscle (compare panels *K* and *H* in Fig. 3). For mice injected with each of three batches of anti-MuSK IgG, pyridostigmine produced statistically significant further reductions in both the area and intensity of endplate AChR clusters in the diaphragm muscle, over and above the effect of anti-MuSK IgG injections (Fig. 4*A*). In the TA muscle the effects of pyridostigmine on endplates were relatively subtle. For mice injected with either AM5 or AM4.4 IgG, pyridostigmine had no measurable effect upon endplate AChR clusters. In the TA muscles of mice injected with AM4.2 IgG, pyridostigmine produced only a modest reduction in AChR cluster area and intensity (Fig. 4*B*). As anticipated, for mice receiving control injections of normal human IgG, pyridostigmine had no effect upon endplate AChR clusters in either the TA or diaphragm muscle (Fig. 4, hatched open bars). Taken together, these results show that, for the therapeutically relevant dose employed, pyridostigmine acted in a muscle-selective way to potentiate the anti-MuSK-induced disassembly of AChR clusters at endplates in the diaphragm muscle.

Changes to synaptic function in the diaphragm muscle after anti-MuSK injections and pyridostigmine treatment

Mice injected with 45 mg day^{-1} AM4.2 IgG or 25 mg day^{-1} AM4.5 IgG for 15 days did not develop overt weakness but displayed, as expected, lower EPP amplitudes than naive control mice (Figs 5*B* and 6*A*). This could be explained by a comparable reduction in quantal amplitude (Figs 5*A* and 6*B*; mEPP amplitude was reduced by 27%, EPP amplitude by 25%). Importantly, when mice injected with AM4.2/4.5 IgG were treated for 1 week with pyridostigmine, both EPP and mEPP amplitudes were further reduced (Figs 5, and 6*A* and *B*; mEPP amplitude was reduced by 45%, EPP amplitude by 47% compared to naive controls). There was no significant difference in resting membrane potential amongst the treatment groups that might account for the observed EPP and mEPP changes (Table 1). The results suggest that pyridostigmine exacerbated reductions in synaptic potentials by lowering the postsynaptic sensitivity to each quantum of ACh.

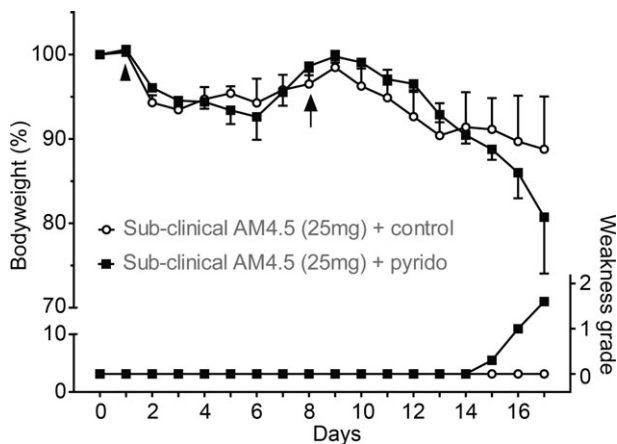


Figure 2. Pyridostigmine treatment can convert subclinical anti-MuSK MG to overt weakness

Average body weights and weakness grades of mice receiving daily injections of AM4.5 IgG (25 mg day^{-1}). A minipump delivering either pyridostigmine (filled squares) or vehicle (open circles) was implanted subcutaneously on day 8 of the anti-MuSK IgG injection series (arrow). Average weakness grade is indicated on the right ordinate. The arrow-head denotes a single injection of cyclophosphamide to suppress any active immune response to the injected human IgG. Data represent the mean \pm SEM for $n = 3$ mice in each treatment group.

Presynaptic effects of anti-MuSK IgG and pyridostigmine

Compared to the marked loss of postsynaptic AChRs, presynaptic effects of anti-MuSK IgG and pyridostigmine were relatively modest. Synaptophysin-stained nerve terminals appeared largely intact in mice injected with anti-MuSK IgG with or without pyridostigmine treatment (Fig. 3). In mice injected with AM5 or AM4.2 we found no significant quantitative changes to the size or staining

intensity of nerve terminals, whether the mice received pyridostigmine or not. The only exception was for NMJs in the TA muscle of those mice that were injected with AM4.4 and treated with pyridostigmine. Nerve terminal area in this particular treatment group was significantly lower than for naive control mice ($P < 0.05$; Supplemental Fig. S3).

Changes in presynaptic transmitter release were also relatively subtle. Injection of anti-MuSK IgG reduced the frequency of spontaneously occurring mEPPs and this reduction was potentiated by pyridostigmine treatment (Fig. 6C). The average number of quanta released in response to nerve stimulation (39.7 ± 2.6 for naive mice) was not reduced significantly by injection of AM4.2/4.5 IgG (33.7 ± 1.4) but the combination of injections of AM4.2/4.5 IgG and treatment with pyridostigmine produced a significant reduction in quantal content

when compared to naive mice (29.4 ± 2.3 ; $P < 0.05$ by ANOVA). Endplates in naive control mice displayed an inverse correlation between the quantal content and mEPP amplitude (Fig. 6D; $P = 0.03$), consistent with previous studies (Plomp *et al.* 1992, 1995; Wang *et al.* 2010; Morsch *et al.* 2012; Viegas *et al.* 2012). In mice injected with AM4.2/4.5 IgG, no such significant correlation could be found ($P = 0.94$; Fig. 6E). Treatment of anti-MuSK-injected mice with pyridostigmine tended to improve this inverse correlation, but not to a statistically significant level ($P = 0.06$; Fig. 6F). Together, these results suggest that the primary effect of both anti-MuSK IgG and pyridostigmine was largely through their action on the postsynaptic response to ACh rather than by presynaptic changes.

The response to quantal release of ACh depends upon the close alignment of tightly packed AChRs immediately

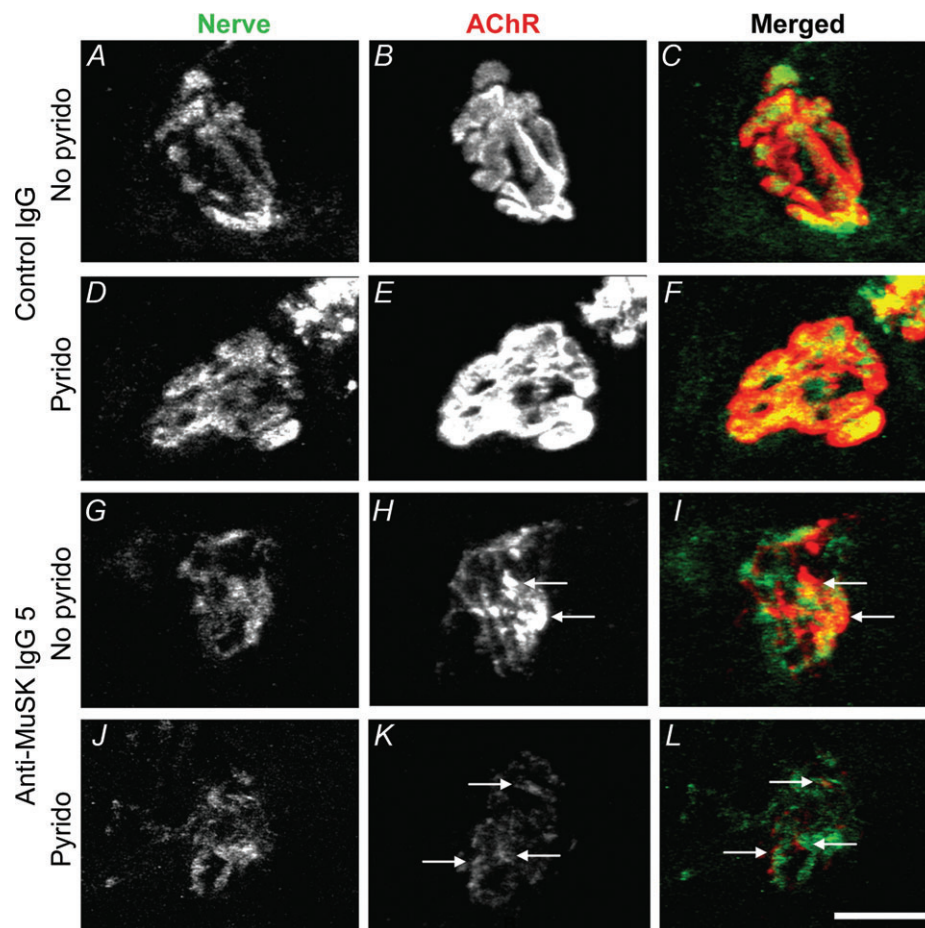


Figure 3. Pyridostigmine potentiates the anti-MuSK-induced loss of endplate AChR

Representative images of NMJs from the diaphragm muscle at the end of the IgG injection series shown in Fig. 1A (day 14). Confocal maximum-projection images from longitudinal sections of the muscle fibres were double labelled for the synaptic vesicle protein synaptophysin (Nerve: panels A, D, G, J) and for postsynaptic AChR (panels B, E, H, K). The right-hand panels show the merged colour images with synaptophysin in green and AChR in red. A–C, motor endplate from a mouse injected with control human IgG and treated with vehicle. D–F, from a mouse injected with control IgG and treated with pyridostigmine. G–I, from a mouse injected with AM5 IgG and treated with vehicle. J–L, from a mouse injected with AM5 IgG and treated with pyridostigmine. Arrows point to AChR cluster fragments within the endplate. Scale bar = 20 μm .

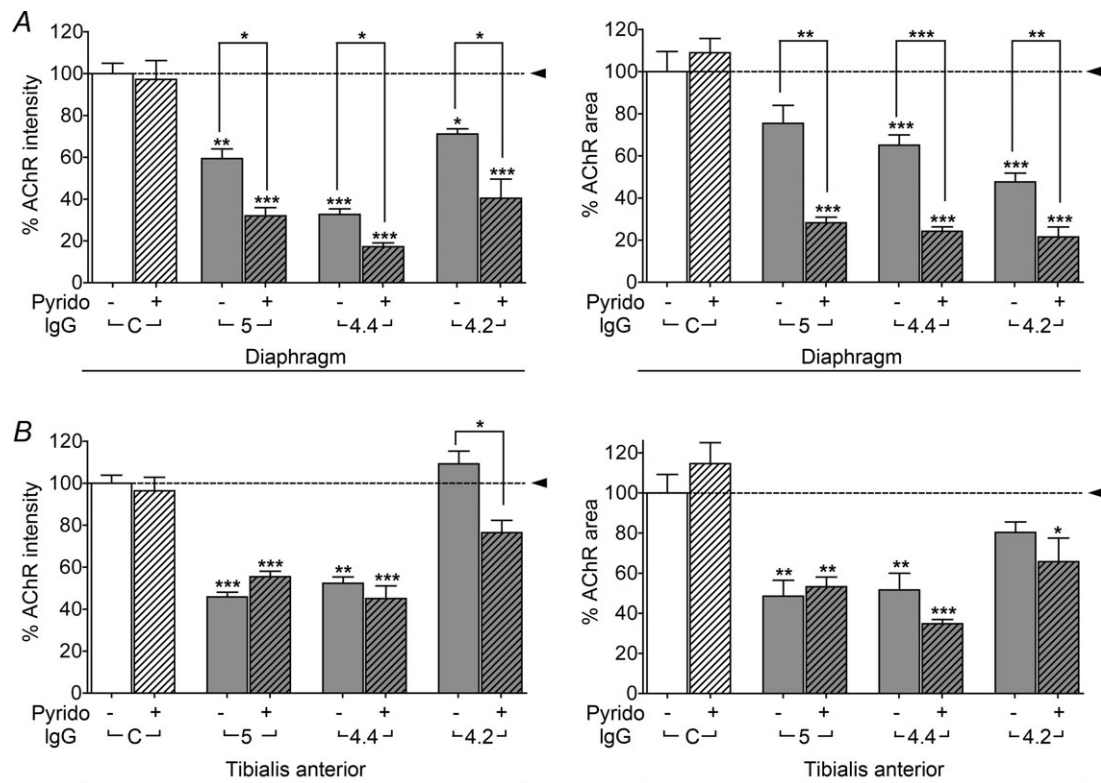


Figure 4. Pyridostigmine potentiates the loss of endplate AChRs in the diaphragm muscle

Bar graphs show the effects of injections of anti-MuSK IgG and pyridostigmine treatment upon the staining intensity and area of endplate AChR clusters. *A*, results for endplates in the diaphragm muscle. *B*, results for the TA muscles 14–15 days after the start of anti-MuSK IgG injections. Subcutaneous minipumps containing pyridostigmine or vehicle were implanted on day 7 or 8, as described in Fig. 1. Grey bars represent mice injected with indicated batches of anti-MuSK IgG (AM 5, 4.2 and 4.4) that were treated with vehicle only. Hatched grey bars show results for mice injected with the indicated batch of anti-MuSK IgG and treated with pyridostigmine for one week (Pyrido +). The horizontal dashed line indicates the mean for control mice that were injected with control human IgG (C) and treated with vehicle alone. Hatched open bars represent mice injected with control human IgG and treated with pyridostigmine. All results were normalised to values for control mice (open bars). Asterisks above bars indicate significant differences compared to control animals within the same experiment. Data represent $n = 3-5$ mice (21–62 endplates sampled per mouse). (* $P < 0.05$; ** $P < 0.01$; *** $P < 0.001$ one-way ANOVA with Bonferroni's correction for multiple comparisons.)

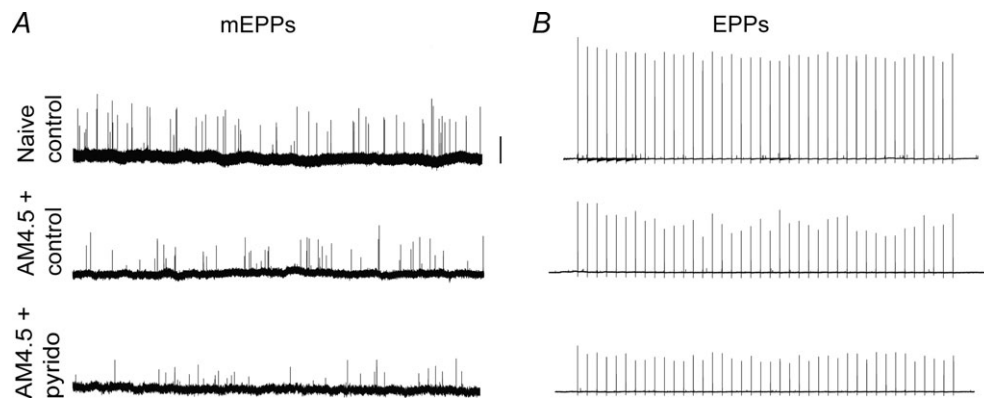


Figure 5. Endplate potential and miniature endplate potential recordings

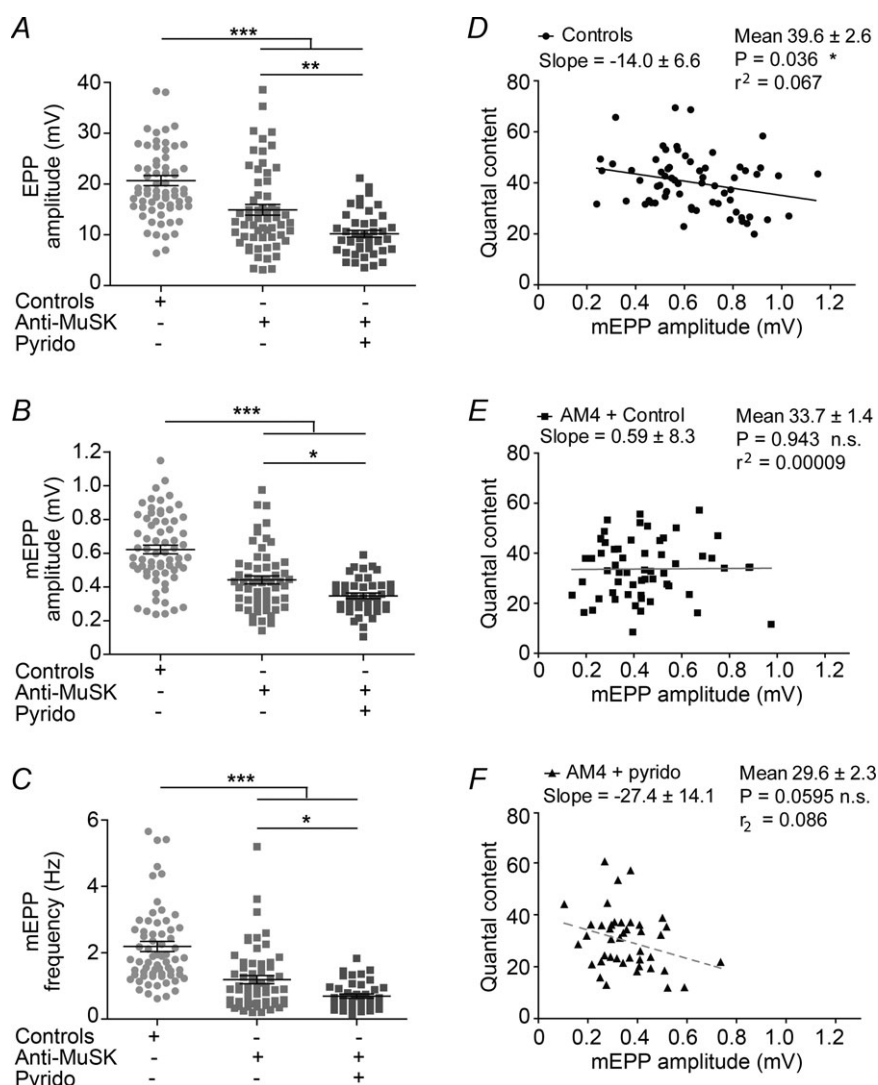
Representative intracellular recordings from fibres in the diaphragm muscle of mice after 15 days of injections with AM4.5 with and without pyridostigmine treatment. *A*, spontaneous miniature endplate potentials (mEPPs) recorded over 60 s (scale bar 0.5 mV). *B*, endplate potentials (EPPs) elicited by phrenic nerve stimulation at 1 stimulus s^{-1} (scale bar 10 mV). These mice never displayed overt muscle weakness, thereby avoiding the possible secondary effects of paralysis.

Table 1. Effects of anti-MuSK and pyridostigmine on synaptic potentials

Parameter	Treatment				
	Naive controls	AM4.2/4.5 IgG + vehicle	AM4.2/4.5 IgG + pyridostigmine	AM4.5 IgG + vehicle	AM4.5 IgG + 3,4-DAP
Number of fibres recorded (mice)	67 (5)	59 (4)	43 (4)	44 (3)	44 (3)
Resting potential (mV)	-65.9 ± 0.4	-67.3 ± 1.1	-66.6 ± 0.6	-68.5 ± 0.8	-67.1 ± 1.9
EPP rise time (ms; 10–90%)	0.72 ± 0.05	0.74 ± 0.16	0.68 ± 0.05	0.93 ± 0.04	0.94 ± 0.06
EPP decay time (ms; 90–10%)	4.81 ± 0.54	4.16 ± 0.05	3.58 ± 0.38	5.05 ± 0.23	5.49 ± 0.45
mEPP rise time (ms; 10–90%)	1.28 ± 0.07	1.17 ± 0.05	1.18 ± 0.07	1.27 ± 0.08	1.43 ± 0.13
mEPP decay time (ms; 10–90%)	4.27 ± 0.18	3.84 ± 0.09	3.89 ± 0.27	4.06 ± 0.29	4.24 ± 0.21

beneath release sites on the presynaptic nerve terminal (Land *et al.* 1981; Sanes & Lichtman, 2001). In control mice AChRs were clustered immediately beneath the greater part of the nerve terminal (Fig. 3C). Injection of anti-MuSK IgG caused the disappearance of AChR clusters from beneath nerve terminals, in both the

diaphragm and TA muscles (Fig. 7; Supplemental Fig. S4). Pyridostigmine potentiated the loss of AChRs from beneath nerve terminals in the diaphragm muscle, but not in the TA muscle (Figs 7 and 3L). Pyridostigmine had no such effect in mice injected with control human IgG (Supplemental Fig. S4).

**Figure 6. Pyridostigmine potentiates anti-MuSK-induced synaptic dysfunction in the diaphragm**

Quantification of endplate potential recordings from muscle fibres in the diaphragm of mice injected with anti-MuSK IgG for 15 days and treated with pyridostigmine or vehicle for the last 7 days. Mice were injected with amounts of anti-MuSK IgG (AM4.2/4.5) that were insufficient to produce whole-body weakness. EPP amplitudes (A), mEPP amplitudes (B) and mEPP frequencies (C) as compared to naive control mice. Anti-MuSK-induced reductions were exacerbated by pyridostigmine treatment. Data represent 42–67 muscle fibres pooled from a total of 4 mice each for the different treatment groups and from 5 control mice (means \pm SEM are given; * $P < 0.05$; ** $P < 0.01$; *** $P < 0.001$ one-way ANOVA, Bonferroni's multiple comparison post test). D, scatter plot showing the inverse relationship between quantal content and mEPP amplitudes among endplates from naive control mice. E, equivalent scatter plot for mice injected with anti-MuSK IgG (AM4.2/4.5) and treated with vehicle. F, scatter plot for mice injected with anti-MuSK IgG (AM4.2/4.5) and treated with pyridostigmine. Data for individual scatter plots were fitted by linear regression. Slope values \pm SEM are shown. Probability values indicated by asterisks reflect the null hypothesis: that the slope values did not deviate from zero.

Interaction between MuSK and acetylcholinesterase

MuSK autoantibodies are reported to disrupt the interaction between MuSK and the collagen Q anchor of synaptic cleft acetylcholinesterase (ColQ) (Kawakami *et al.* 2011). We therefore stained NMJs in the diaphragm muscles for acetylcholinesterase with Alexa647-Fasciculin 2 (Krejci *et al.* 2006; Fig. 8A). In mice

that became weak after injections of AM4.4 IgG for 15 days endplate AChE staining was reduced in similar proportion to AChR staining (Fig. 8B). However while pyridostigmine treatment exacerbated the loss of endplate AChR, it had no such effect on endplate AChE staining (Fig. 8C).

Pyridostigmine exacerbates anti-MuSK-induced redistribution of endplate AChRs

Maximum projection images, transverse to the muscle fibre axis, provide a way to detect the dimly stained remnants of an endplate AChR plaque and dispersed peri-synaptic AChR. In these images normal endplates appear as intensely stained crescent-shaped AChR clusters with sharp boundaries wrapped around the outer face of the muscle fibre (Fig. 9A, 'type a' AChR pattern). In the diaphragm muscles of mice injected for 14–15 days with anti-MuSK IgG some AChR clusters were accompanied by a ring of diffuse AChR staining and scattered puncta spread right around the muscle fibre circumference (Fig. 9B arrows, 'type b' fibre profile). Other fibre profiles revealed only a dim AChR cluster with or without a visible ring of diffuse staining (Fig. 9C, 'type c'). Profiles of some fibres revealed nothing but the ring of diffuse AChR staining and scattered puncta (Fig. 9D, 'type d'). The diaphragm muscle of control mice displayed nothing but the 'type a' AChR pattern. Injection of either AM5 or AM4.4 was sufficient on its own to virtually eliminate 'type a' fibre profiles. They were replaced by mainly dispersed, 'type c' and 'type d' AChR patterns. Injection of AM4.2 IgG caused changes that were less severe. The diaphragm muscle retained 29% 'type a' healthy AChR clusters. In the latter context treatment with pyridostigmine was able to exacerbate the reduction in 'type a' fibre profiles (from 29% to 3%; Fig. 9G; $P = 0.019$, unpaired *t* test, two-tailed, $n = 3$ mice per group).

3,4-Diaminopyridine enhances neuromuscular transmission

We next investigated the impact of 3,4-DAP to see whether a drug that enhances presynaptic ACh release (rather than the persistence of ACh in the synaptic cleft) would also exacerbate AChR loss in our model of anti-MuSK MG. Like pyridostigmine, 3,4-DAP increases ACh in the synaptic cleft. Unlike pyridostigmine, 3,4-DAP acts via a presynaptic increase of quantal release. Mice received injections of AM4.5 sufficient to produce weakness over a 15 day period (35 mg IgG per day; Fig. 10A). Treatment with 3,4-DAP ($8 \text{ mg kg}^{-1} \text{ day}^{-1}$) from days 8 to 15 did not affect the onset of weight loss and generalised weakness over the 15 day treatment (Fig. 10A). Thus 3,4-DAP neither accelerated nor mitigated disease onset. In *ex vivo* preparations of the diaphragm muscle the

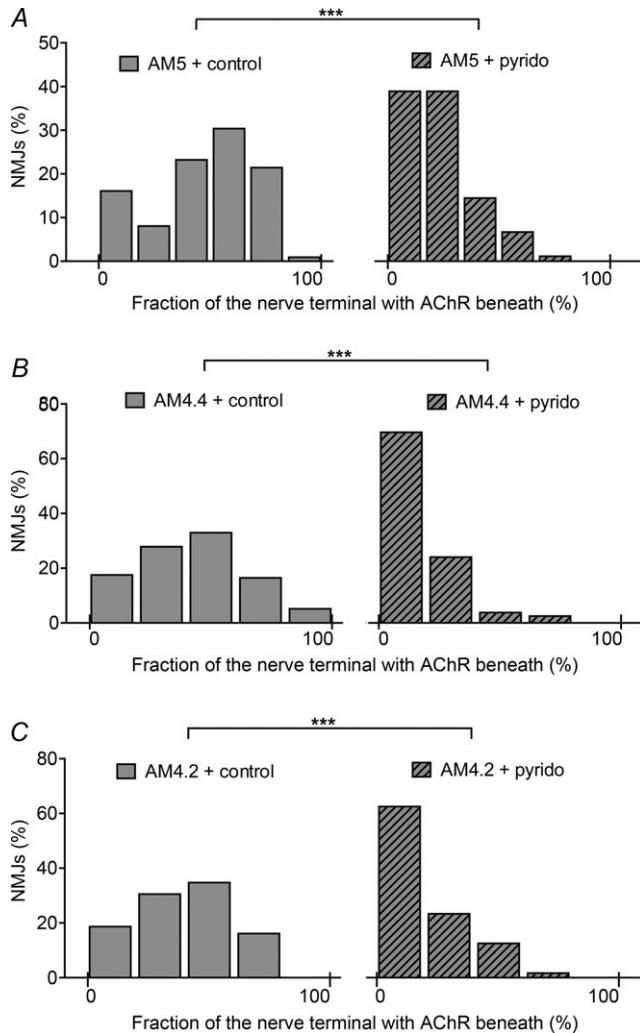


Figure 7. Pyridostigmine exacerbates the loss of AChRs from beneath nerve terminals in the diaphragm

Frequency histograms show the percentage of the nerve terminal that had postsynaptic AChR clusters aligned beneath it. These histograms demonstrate the effect of pyridostigmine treatment in mice injected with anti-MuSK IgG. A full set of distributions comparing all the treatment groups are shown in Supplemental Fig. S5. A, results of mice injected with AM5 IgG with and without pyridostigmine treatment. B, results for mice injected with AM4.4 with and without pyridostigmine. C, results for mice injected with AM4.2 IgG with and without pyridostigmine. Each histogram represents 60–122 endplates pooled from 3 mice after 14 days of anti-MuSK IgG injections and 7 days of treatment with either pyridostigmine or vehicle (** $P < 0.001$, Kruskal-Wallis Dunn's multiple comparison post test).

CMAP amplitude showed a decrement upon repetitive stimulation of the phrenic nerve. Mice that had received systemic 3,4-DAP treatment did not display this decrement in CMAP amplitudes (Fig. 10B). Their endplates also showed an upward trend in the area of AChRs and nerve terminals although these differences did not reach significance (Fig. 10C and D). There was no change in alignment of AChRs with nerve terminals (Fig. 10E). Treatment with 3,4-DAP significantly increased both quantal content and EPP amplitude but the frequency and amplitude of mEPPs were not affected (Fig. 11A). As noted above injections of anti-MuSK IgG disrupted the inverse relationship between the quantal amplitude of an endplate and its quantal content. Interestingly, treatment with 3,4-DAP restored the inverse relationship (Fig. 11B). Thus, unlike pyridostigmine, 3,4-DAP treatment did not potentiate the structural and functional impairment of the endplate that was initiated by anti-MuSK patient antibodies.

Discussion

In our mouse model of anti-MuSK MG, pyridostigmine exacerbated the autoantibody-induced loss of endplate AChR clusters particularly in the diaphragm muscle,

thereby exacerbating reduced synaptic function. In mice where the injection of anti-MuSK IgG *per se* was not quite sufficient to produce weakness, pyridostigmine treatment for 9 days was capable of precipitating severe weakness. The therapeutically relevant levels of pyridostigmine employed were not sufficient to produce signs of toxicity or NMJ changes in the absence of anti-MuSK IgG injections. In contrast to pyridostigmine, 3,4-DAP treatment for 1 week improved synaptic function without worsening endplate AChR loss. Thus pyridostigmine (or the persistence of ACh in the synaptic cleft that pyridostigmine produces) appears to act synergistically with anti-MuSK IgG to accelerate AChR cluster disassembly, particularly at NMJs in the diaphragm muscle.

Cholinesterase inhibitors act to prolong and enhance the activation of endplate AChR channels (Fedorov, 1976; Albuquerque *et al.* 1984), but excessive or long-term treatment with such drugs has been reported to cause structural and functional impairment to the NMJ (Chang *et al.* 1973; Engel *et al.* 1973; Hudson *et al.* 1985, 1986; Drake-Baumann & Seil, 1999). When otherwise healthy rats received prostigmine for several months, NMJs of the diaphragm muscle were more affected than those of the gastrocnemius muscle (Engel *et al.* 1973). Patients with inherited deficiency of junctional AChE also suffer from long-term pre- and postsynaptic impairments and

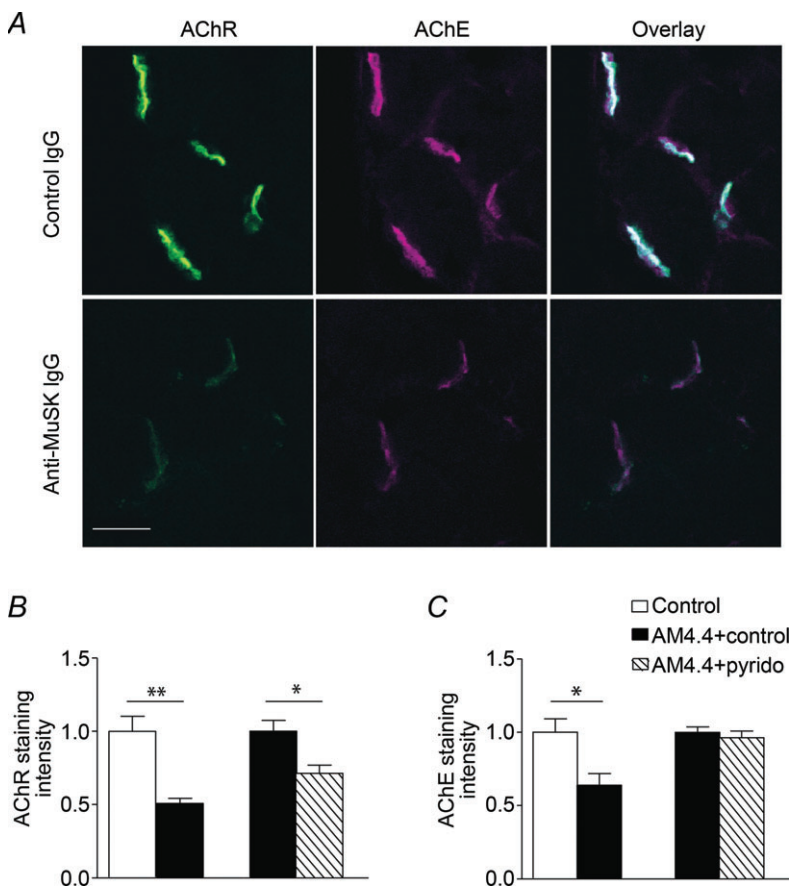


Figure 8. Reduced endplate AChE immunoreactivity in the diaphragm muscle after injections of anti-MuSK IgG

Mice were injected daily for 15 days with either control human IgG (open bars) or AM4.4 IgG and were treated with pyridostigmine or vehicle for the last 7 days. A, transverse optical sections of the diaphragm double labelled for AChR (with Alexa488- α -BGT) and AChE (with Alexa647-Fasciculin 2). Right-hand panels show the merge of the two fluorescence channels. The brightness and contrast was increased to the same degree for all panels to permit reproduction of the dim residual staining of anti-MuSK IgG-injected mice. Scale bar is 20 μ m. B and C, quantification of the intensity of endplate staining for AChR (B) and AChE (C). Treatment groups are indicated in panel C. Pairs of bars compare the effect of anti-MuSK IgG (filled versus open bars) and treatment with pyridostigmine after anti-MuSK IgG injection (hatched versus filled bar). With each pair of bars the right-hand bar is normalised to the left-hand bar. Anti-MuSK IgG reduced both AChR and AChE staining intensity. Pyridostigmine potentiated the reduction of endplate AChR staining but not the reduction in AChE staining. Each bar represents mean \pm SEM for $n = 3$ mice (* $P < 0.05$; ** $P < 0.01$; unpaired Student's t test).

eventual failure of neuromuscular transmission (Engel & Sine, 2005). Our aim was to test the impact of therapeutically relevant levels of cholinesterase inhibition in the context of anti-MuSK MG in an established mouse model, because clinical experience from afflicted patients suggested lack of pyridostigmine efficacy. Oral doses of pyridostigmine in MG patients typically range from 180 to 360 mg day⁻¹. In one report, the best effective stable dose of pyridostigmine for each patient was found to be that which reduced the individual's blood AChE activity by 45–65% (Henze *et al.* 1991). We implanted subcutaneous minipumps to provide a steady infusion of pyridostigmine that reduced blood cholinesterase activity by a slightly lesser degree ($39 \pm 4\%$ reduction). Consistent with a muscle-selective action, we found that pyridostigmine treatment exacerbated anti-MuSK-induced impairment to NMJs predominantly in the diaphragm muscle and with little effect in the TA. Thus levels of cholinesterase inhibition that were not harmful in the mouse *per se*, selectively exacerbated anti-MuSK MG in the diaphragm muscle.

Previous studies showed that MuSK autoantibodies caused reductions both in mEPP amplitude and frequency (Klooster *et al.* 2012; Mori *et al.* 2012b; Morsch *et al.* 2012;

Viegas *et al.* 2012). One study also found a significant reduction in quantal content (Mori *et al.* 2012b). In the present work we found a significant reduction in quantal content, but only in mice injected with anti-MuSK IgG that also received pyridostigmine treatment. Pyridostigmine also exacerbated the anti-MuSK-induced reduction in mEPP frequency. However, since anti-MuSK injections caused the disappearance of AChR from beneath large parts of the nerve terminal and this loss was potentiated by pyridostigmine the apparent decrease in mEPP frequency may be interpreted in a different way. According to the saturated disc model of neuromuscular transmission, even after complete block of esterases, each quantum of acetylcholine activates only those postsynaptic AChRs within a small circle (less than one micrometre in diameter), centred on the exocytotic pore (Land *et al.* 1981). Thus AChRs must be clustered immediately beneath the transmitter release site. We suggest that it is possible that the structurally normal appearing nerve terminals may have continued to release quanta, but onto parts of the endplate denuded of AChR. Therefore some of the released quanta may not have contributed to detectable mEPPs.

3,4-DAP improves transmitter release from the nerve terminal and is clinically used in some

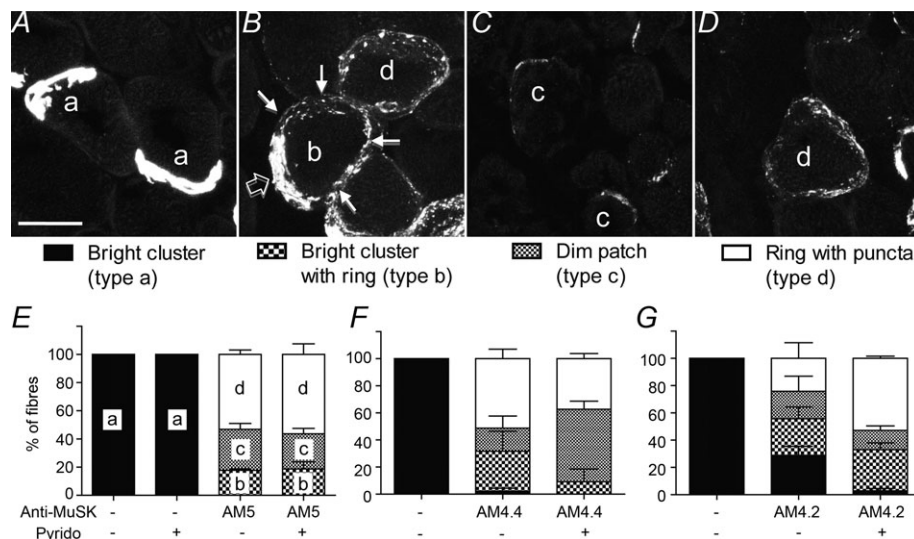


Figure 9. Increased dispersal of the endplate AChR clusters after pyridostigmine treatment

Transverse confocal maximum-projection images of the diaphragm muscle were stained for endplate AChR. AChR-positive fibre profiles were counted by an observer who was blinded to the treatment groups. Four different types of AChR staining were defined. A, normal, intensely stained crescent-shaped endplate AChR clusters from a control mouse (named 'type a'). B–D, abnormal AChR staining patterns in mice after 14 days of injections with anti-MuSK IgG. B, an endplate AChR cluster with a ring of diffuse sarcolemmal AChR staining (labelled 'type b' pattern). Arrows point to the ring staining. A neighbouring fibre shows only the ring of AChR staining ('type d' pattern). C, muscle fibres showing only a dim patch of AChR staining ('type c'). D, another example of a diffuse ring of sarcolemmal AChR staining ('type d'). E–G, percentages of each type of AChR-positive staining pattern (a, b, c and d) sampled from diaphragm muscles. E, results for mice injected with AM5 IgG or control human IgG, with and without pyridostigmine treatment. F, results for mice injected with AM4.4 IgG, with and without pyridostigmine treatment. The first bar represents control (naive) mice. G, results for mice injected with AM4.2 IgG, with and without pyridostigmine treatment. These mice did not become weak. The first bar represents naive control mice. Error bars represent the SEM for $n = 3$ mice. Brightness and contrast were increased uniformly over all images to facilitate reproduction. Scale bar in A is 20 μm.

congenital myasthenic syndromes and in patients with Lambert–Eaton myasthenic syndrome (Titulaer *et al.* 2011). The immediate, acute effect of 3,4-DAP injection into MuSK-immunised mice was to increase CMAP and EPP amplitudes (Mori *et al.* 2012a). The effect of chronic treatment has not been previously studied in any model of anti-MuSK MG. Aminopyridines such as 3,4-DAP increase the quantal content without altering the amplitude or duration of the response to individual quanta (Thomsen & Wilson, 1983; Hong & Chang, 1990; Giovannini *et al.* 2002). Treatment of our anti-MuSK-injected mice with 3,4-DAP for 1 week

increased quantal content as expected but, in contrast to pyridostigmine, did not exacerbate anti-MuSK-induced reductions in AChR density and EPP amplitude. Rather, 3,4-DAP enhanced the EPP amplitude and preserved the inverse relationship between the quantal content of an endplate and its quantal amplitude.

By what mechanism might pyridostigmine potentiate the process of AChR cluster dispersal that is instigated by anti-MuSK IgG? During embryonic development a signalling pathway involving neural agrin, Lrp4, MuSK and rapsyn promotes the growth of post-synaptic AChR clusters (Wu *et al.* 2010; Ghazanfari

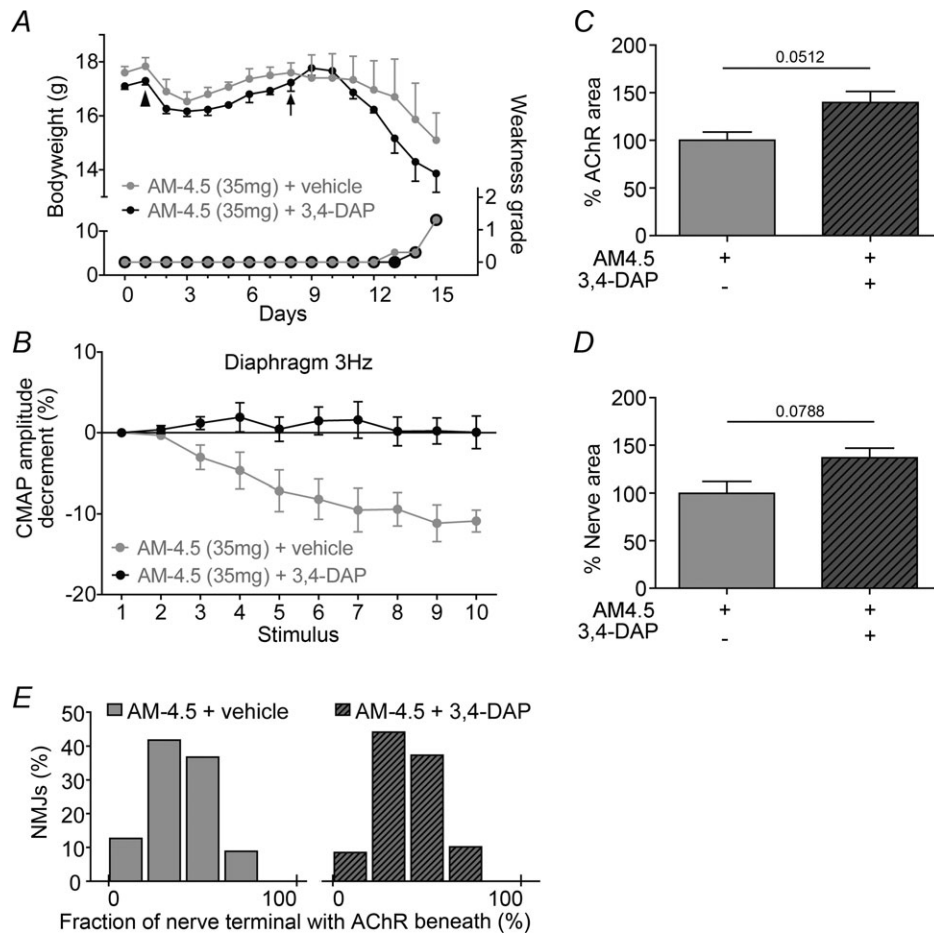


Figure 10. Effects of 3,4-diaminopyridine treatment on the NMJ after passive transfer of MuSK antibodies

A, average body weights and weakness grades of mice receiving daily injections of AM4.5 IgG (35 mg day⁻¹). The arrow indicates subcutaneous implantation of a minipump delivering 3,4-DAP at a rate of 8 mg kg⁻¹ day⁻¹ (black circles) or vehicle (grey circles). The arrowhead denotes a single injection of cyclophosphamide. Treatment with 3,4-DAP had no effect upon the loss of body weight (left-hand ordinate) and onset of whole-body weakness (symbols in lower part of panel and right-hand ordinate). B, mean CMAP amplitudes in the isolated diaphragm muscle during repetitive stimulation of the phrenic nerve (3 stimuli s⁻¹). Injections of AM4.5 produced a decrement in CMAP amplitude (grey filled circles) but no such decrement was seen in mice treated with 3,4-DAP (black circles). C and D, effects of 3,4-DAP upon the area of endplate AChR clusters (C), and presynaptic nerve terminal (D) at endplates in the diaphragm of mice injected with anti-MuSK IgG (AM4.5). Data represent the mean \pm SEM for $n = 3$ mice in each treatment group (unpaired Student's *t* test). E, frequency distributions showing the degree of nerve terminal–AChR alignment at endplates of mice injected with anti-MuSK IgG (AM4.5) and treated with either 3,4-DAP or vehicle.

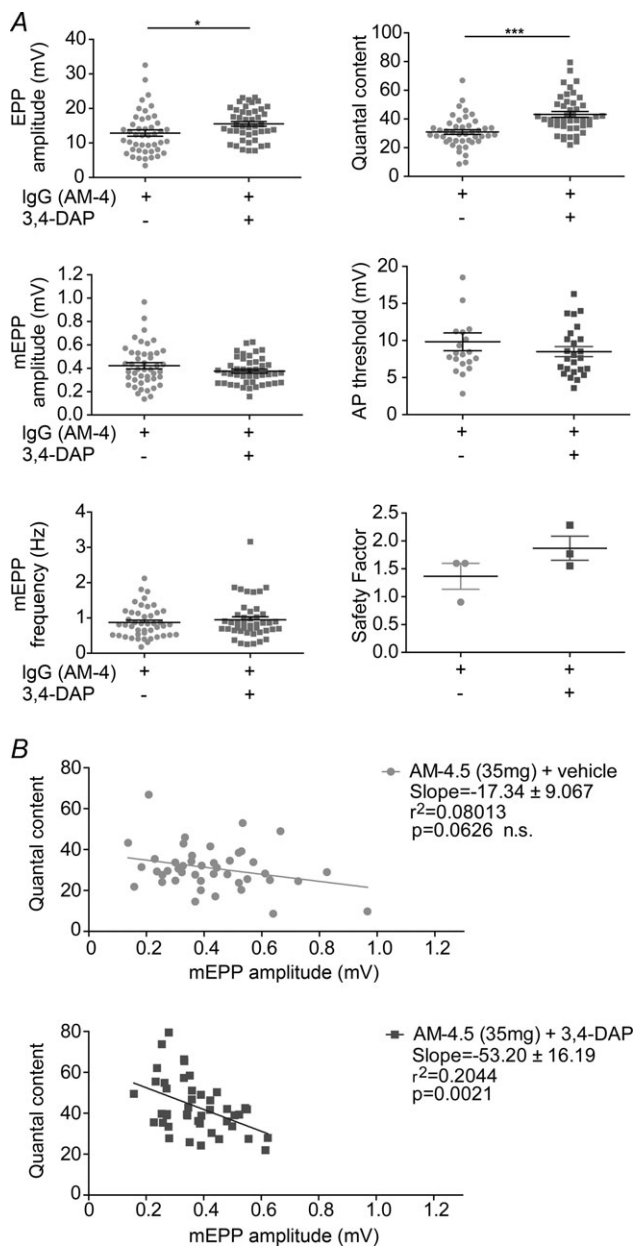


Figure 11. Increased endplate potential amplitudes in mice treated with 3,4-DAP

Quantification of endplate potential recordings from muscle fibres in the diaphragm of mice injected with AM4.5 IgG for 15 days and treated with pyridostigmine or vehicle for the last 7 days. **A**, electrophysiological parameters. EPP amplitudes and quantal content were significantly greater in anti-MuSK-injected mice that were treated with 3,4-DAP, compared to those treated with vehicle only (* $P < 0.05$; *** $P < 0.001$ unpaired Student's t test). **B**, the normal inverse relationship between quantal content and quantal amplitude was lost in mice injected with AM4.5 (upper scatter plot) but the inverse relationship was strengthened in mice treated with 3,4-DAP (lower scatter plot). Results represent 45 muscle fibres pooled from a total of 3 mice for each treatment group. Scatter plots were fitted by linear regression. Slope values \pm SEM are shown. Probability values indicated by asterisks reflect the significance of rejecting the null hypothesis that the slope values do not deviate from zero.

et al. 2011). Acetylcholine on the other hand appears to activate a pathway involving subsynaptic AChRs, inositol-1,4,5-trisphosphate receptors, calcium, calpain and cyclin-dependent kinase-5 to disassemble AChR clusters (Lin *et al.* 2005; Misgeld *et al.* 2005; Zhu *et al.* 2011). The MuSK pathway may stabilise endplate AChR clusters by inhibiting the AChR cluster disassembly pathway at the healthy endplate (Misgeld *et al.* 2005; Chen *et al.* 2007). It has been proposed that the balance of these two interacting pathways helps to sculpt the developing NMJ (Ono, 2008). AChR channelopathies that greatly prolong the local calcium influx in response to each quantum of ACh caused AChR cluster disassembly (Zhu *et al.* 2011). Pyridostigmine also increases the duration of each quantal current, albeit to a lesser extent (Pascuzzo *et al.* 1984). Under conditions where MuSK function is impaired by autoantibodies, perhaps the prolongation of local calcium influx by pyridostigmine is sufficient to drive AChR cluster disassembly. The modest level of cholinesterase inhibition employed in the present study did not significantly affect endplate AChR clusters. However, the same dosage caused marked AChR loss and functional impairment in mice injected with anti-MuSK IgG where the AChR cluster-stabilising role of MuSK was impaired. The balance of MuSK and ACh signalling may thus be a critical determinant of the size and functionality of the adult NMJ.

MuSK autoantibodies can disrupt the interaction between MuSK and the collagenic tail subunit of synaptic cleft acetylcholinesterase (ColQ) (Kawakami *et al.* 2011). Mori *et al.* reported a 35% reduction in the AChE-stained area of endplates in the soleus muscle of mice that became weak after immunisation with MuSK (Mori *et al.* 2012b). This could be important because loss of endplate AChE would be expected to potentiate any harmful prolonged activation of endplate AChRs in the manner discussed above. In our mice that became weak after injection with anti-MuSK IgG, the intensity of AChE staining at endplates in the diaphragm muscle was 36% lower compared to control mice. Pyridostigmine treatment caused no additional change in endplate AChE staining intensity. Mori and colleagues reported that active immunisation with MuSK prolonged the decay time of the EPP (Mori *et al.* 2012b), but our anti-MuSK injections did not (Table 1). It remains possible that endplate AChE was affected more in the actively immunised mice than in the mice injected with anti-MuSK IgG. Differing analytical methods preclude direct comparison of the percentage reductions in endplate AChE. Moreover, Mori *et al.* reported their AChE reduction for endplates of the soleus muscle, rather than the diaphragm. In addition, the average reduction we found in endplate AChE staining might not reflect the subset of fibres from which we recorded EPPs. The anti-MuSK injection series caused an increase in the fraction of fibre impalements from

which no EPPs could be recorded (Morsch *et al.* 2012). Silent/paralysed fibres undergo a rapid reduction in junctional cholinesterase (Sketelj *et al.* 1993), but they would not contribute to our EPP records.

It remains uncertain why the diaphragm muscle should be particularly vulnerable to the exacerbation of anti-MuSK MG by pyridostigmine. Certain muscles (including the diaphragm) appear to be affected more by anti-MuSK IgG than others (including the TA), possibly due to quantitative differences in the expression of MuSK (Xu *et al.* 2006; Cole *et al.* 2010; Punga *et al.* 2011). Endplates in the diaphragm were also more susceptible to long-term cholinesterase inhibition than those in the gastrocnemius muscle (Engel *et al.* 1973). Conceivably the greater sensitivity of the diaphragm to pyridostigmine might relate to its more regular duty cycle or to subtle molecular differences between motor endplates in different muscles of the body.

Pyridostigmine remains the only approved symptomatic drug for the treatment of MG. Yet one week of treatment was enough to exacerbate neuromuscular impairment in our mouse model of MuSK-MG. In the same anti-MuSK model one week of treatment with 3,4-DAP significantly enhanced neuromuscular transmission without exacerbating loss of endplate AChRs. Any short-term beneficial effect of pyridostigmine may simply obscure its longer-term deleterious effects on the motor endplate. It will be important for all forms of myasthenia to evaluate whether cholinesterase therapy might cause selective harm to certain muscles such as the diaphragm that are clinically more difficult to evaluate *in vivo*.

References

- Albuquerque E, Akaike A, Shaw K & Rickett D (1984). The interaction of anticholinesterase agents with the acetylcholine receptor-ionic channel complex. *Fundam Appl Toxicol* **4**, S27–33.
- Banwell BL, Ohno K, Sieb JP & Engel AG (2004). Novel truncating RAPSN mutations causing congenital myasthenic syndrome responsive to 3,4-diaminopyridine. *Neuromuscul Disord* **14**, 202–207.
- Bromann PA, Zhou H & Sanes JR (2004). Kinase- and rapsyn-independent activities of the muscle specific kinase (MuSK). *Neuroscience* **125**, 417–426.
- Chang CC, Chen TF & Chuang ST (1973). Influence of chronic neostigmine treatment on the number of acetylcholine receptors and the release of acetylcholine from the rat diaphragm. *J Physiol* **230**, 613–618.
- Chen F, Qian L, Yang Z-H, Huang Y, Ngo ST, Ruan N-J, Wang J, Schneider C, Noakes PG, Ding YQ, Mei L & Luo ZG (2007). Rapsyn interaction with calpain stabilizes AChR clusters at the neuromuscular junction. *Neuron* **55**, 247–260.
- Chroni E & Punga AR (2012). Neurophysiological characteristics of MuSK antibody positive myasthenia gravis mice: Focal denervation and hypersensitivity to acetylcholinesterase inhibitors. *J Neurol Sci* **316**, 150–157.
- Cole RN, Ghazanfari N, Ngo ST, Gervasio OL, Reddel SW & Phillips WD (2010). Patient autoantibodies deplete postsynaptic muscle specific kinase leading to disassembly of the ACh receptor scaffold and myasthenia gravis in mice. *J Physiol* **588**, 3217–3229.
- Cole RN, Reddel SW, Gervasio OL & Phillips WD (2008). Anti-MuSK patient antibodies disrupt the mouse neuromuscular junction. *Ann Neurol* **63**, 782–789.
- Drachman DB (1994). Myasthenia gravis. *N Engl J Med* **330**, 1797–1810.
- Drachman DB, Angus CW, Adams RN, Michelson JD & Hoffman GJ (1978). Myasthenic antibodies cross-link acetylcholine receptors to accelerate degradation. *New Eng J Med* **298**, 1116–1122.
- Drake-Baumann R & Seil FJ (1999). Effects of exposure to low-dose pyridostigmine on neuromuscular junctions *in vitro*. *Muscle Nerve* **22**, 696–703.
- Drummond GB (2009). Reporting ethical matters in *The Journal of Physiology*: standards and advice. *J Physiol* **587**, 713–719.
- Engel AG, Lambert EH & Howard FM (1977). Immune complexes (IgG and C3) at the motor end-plate in myasthenia gravis: ultrastructural and light microscopic localization and electrophysiologic correlations. *Mayo Clin Proc* **52**, 267–280.
- Engel AG, Lambert EH & Santa T (1973). Study of long-term anticholinesterase therapy. *Neurology* **23**, 1273–1281.
- Engel AG & Sine SM (2005). Current understanding of congenital myasthenic syndromes. *Curr Opin Pharmacol* **5**, 308–321.
- Evoli A, Tonali PA, Padua L, Monaco ML, Scuderi F, Batocchi AP, Marino M & Bartoccioni E (2003). Clinical correlates with anti-MuSK antibodies in generalized seronegative myasthenia gravis. *Brain* **126**, 2304–2311.
- Fedorov VV (1976). Effect of cholinesterase inhibitors on synaptic potentials of the frog neuromuscular junction. *Neurosci Behav Physiol* **7**, 201–206.
- Gervasio OL & Phillips WD (2005). Increased ratio of rapsyn to ACh receptor stabilizes postsynaptic receptors at the mouse neuromuscular synapse. *J Physiol* **562**, 673–685.
- Ghazanfari N, Fernandez KJ, Murata Y, Morsch M, Ngo ST, Reddel SW, Noakes PG & Phillips WD (2011). Muscle specific kinase: Organiser of synaptic membrane domains. *Int J Biochem Cell Biol* **43**, 295–298.
- Giovannini F, Sher E, Webster R, Boot J & Lang B (2002). Calcium channel subtypes contributing to acetylcholine release from normal, 4-aminopyridine-treated and myasthenic syndrome auto-antibodies-affected neuromuscular junctions. *Br J Pharmacol* **136**, 1135–1145.
- Glass DJ, Bowen DC, Stitt TN, Radziejewski C, Brunno J, Ryan TE, Gies DR, Shah S, Mattsson K, Burden SJ, DiStefano PS, Valenzuela DM, DeChiara TM & Yancopoulos GD (1996). Agrin acts via a MuSK receptor complex. *Cell* **85**, 513–523.
- Gomez AM, Van Den Broeck J, Vrolix K, Janssen SP, Lemmens MA, Van Der Esch E, Duimel H, Frederik P, Molenaar PC, Martínez-Martínez P, De Baets MH & Losen M (2010). Antibody effector mechanisms in myasthenia gravis-pathogenesis at the neuromuscular junction. *Autoimmunity* **43**, 353–370.

- Haigh JR, Lefkowitz LJ, Capacio BR, Doctor BP & Gordon RK (2008). Advantages of the WRAIR whole blood cholinesterase assay: Comparative analysis to the micro-Ellman, Test-mate ChETM, and Michel (Δ pH) assays. *Chem Biol Interact* **175**, 417–420.
- Hatanaka Y, Hemmi S, Morgan MB, Scheufele ML, Claussen GC, Wolfe GI & Oh SJ (2005). Nonresponsiveness to acetylcholinesterase agents in patients with MuSK-antibody-positive MG. *Neurology* **65**, 1508–1509.
- Henze T, Nenner M & Michaelis HC (1991). Determination of erythrocyte-bound acetylcholinesterase activity for monitoring pyridostigmine therapy in myasthenia gravis. *J Neurol* **238**, 225–229.
- Hesser BA, Henschel O & Witzemann V (2006). Synapse disassembly and formation of new synapses in postnatal muscle upon conditional inactivation of MuSK. *Mol Cell Neurosci* **31**, 470–480.
- Hoch W, McConville J, Helms S, Newsom-Davis J, Melms A & Vincent A (2001). Autoantibodies to the receptor tyrosine kinase MuSK in patients with myasthenia gravis without acetylcholine receptor antibodies. *Nat Med* **7**, 365–368.
- Hong SJ & Chang CC (1990). Facilitation by 3,4-diaminopyridine of regenerative acetylcholine release from mouse motor nerve. *Br J Pharmacol* **101**, 793–798.
- Hudson CS, Foster RE & Kahng MW (1985). Neuromuscular toxicity of pyridostigmine bromide in the diaphragm, extensor digitorum longus, and soleus muscles of the rat. *Fundam Appl Toxicol* **5**, S260–S269.
- Hudson CS, Foster RE & Kahng MW (1986). Ultrastructural effects of pyridostigmine on neuromuscular junctions in rat diaphragm. *Neurotoxicol* **7**, 167–186.
- Jha S, Xu K, Maruta T, Oshima M, Mosier DR, Atassi MZ & Hoch W (2006). Myasthenia gravis induced in mice by immunization with the recombinant extracellular domain of rat muscle-specific kinase (MuSK). *J Neuroimmunol* **175**, 107–117.
- Kawakami Y, Ito M, Hirayama M, Sahashi K, Ohkawara B, Masuda A, Nishida H, Mabuchi N, Engel AG & Ohno K (2011). Anti-MuSK autoantibodies block binding of collagen Q to MuSK. *Neurology* **77**, 1–8.
- Kim N, Stiegler AL, Cameron TO, Hallock PT, Gomez AM, Huang JH, Hubbard SR, Dustin ML & Burden SJ (2008). Lrp4 is a receptor for agrin and forms a complex with MuSK. *Cell* **135**, 334–342.
- Klooster R, Plomp JJ, Huijbers MG, Niks EH, Straasheijm KR, Detmers FJ, Hermans PW, Sleijpen K, Verrips A, Losen M, Martinez-Martinez P, De Baets MH, van der Maarel S & Verschuuren JJ (2012). Muscle-specific kinase myasthenia gravis IgG4 autoantibodies cause severe neuromuscular junction dysfunction in mice. *Brain* **135**, 1081–1101.
- Kong XC, Barzaghi P & Ruegg MA (2004). Inhibition of synapse assembly in mammalian muscle *in vivo* by RNA interference. *EMBO Rep* **5**, 183–188.
- Krejci E, Valenzuela IM-P, Ameziane R & Akaaboune M (2006). Acetylcholinesterase dynamics at the neuromuscular junction of live animals. *J Biol Chem* **281**, 10347–10354.
- Land BR, Salpeter EE & Salpeter MM (1981). Kinetic parameters for acetylcholine interaction in intact neuromuscular junction. *Proc Natl Acad Sci U S A* **78**, 7200–7204.
- Lin W, Dominguez B, Yang J, Aryal P, Brandon EP, Gage FH & Leem K-F (2005). Neurotransmitter acetylcholine negatively regulates neuromuscular synapse formation by a Cdk5-dependent mechanism. *Neuron* **46**, 569–579.
- Misgeld T, Kummer TT, Lichtman JW & Sanes JR (2005). Agrin promotes synaptic differentiation by counteracting an inhibitory effect of neurotransmitter. *Proc Natl Acad Sci U S A* **102**, 11088–11093.
- Mori S, Kishi M, Kubo S, Akiyoshi T, Yamada S, Miyazaki T, Konishi T, Maruyama N & Shigemoto K (2012a). 3,4-Diaminopyridine improves neuromuscular transmission in a MuSK antibody-induced mouse model of myasthenia gravis. *J Neuroimmunol* **245**, 75–78.
- Mori S, Kubo S, Akiyoshi T, Yamada S, Miyazaki T, Hotta H, Desaki J, Kishi M, Konishi T, Nishino Y, Miyazawa A, Maruyama N & Shigemoto K (2012b). Antibodies against muscle-specific kinase impair both presynaptic and postsynaptic functions in a murine model of myasthenia gravis. *Am J Pathol* **180**, 798–810.
- Mori S, Yamada S, Kubo S, Chen J, Matsuda S, Shudou M, Maruyama N & Shigemoto K (2012c). Divalent and monovalent autoantibodies cause dysfunction of MuSK by distinct mechanisms in a rabbit model of myasthenia gravis. *J Neuroimmunol* **244**, 1–7.
- Morsch M, Reddel SW, Ghazanfari N, Toyka KV & Phillips WD (2012). Muscle specific kinase autoantibodies cause synaptic failure through progressive wastage of postsynaptic acetylcholine receptors. *Exp Neurol* **237**, 286–295.
- Ono F (2008). An emerging picture of synapse formation: a balance of two opposing pathways. *Sci Signal* **1**, pe3.
- Pascuzzo GJ, Akaike A, Maleque MA, Shaw KP, Aronstam RS, Rickett DL & Albuquerque EX (1984). The nature of the interactions of pyridostigmine with the nicotinic acetylcholine receptor-ionic channel complex. I. Agonist, desensitizing, and binding properties. *Mol Pharmacol* **25**, 92–101.
- Plomp JJ, van Kempen GTH, DeBaets M, Graus YMF, Kuks JBM & Molenaar PC (1995). Acetylcholine release in myasthenia gravis: regulation at single end-plate level. *Ann Neurol* **37**, 627–636.
- Plomp JJ, van Kempen GTH & Molenaar PC (1992). Adaptation of quantal content to decreased postsynaptic sensitivity at single endplates in α -bungarotoxin-treated rats. *J Physiol* **458**, 487–499.
- Punga AR, Lin S, Oliveri F, Meinen S & Ruegg MA (2011). Muscle-selective synaptic disassembly and reorganization in MuSK antibody-positive MG mice. *Exp Neurol* **230**, 207–217.
- Richman DP & Agius MA (2003). Treatment of autoimmune myasthenia gravis. *Neurology* **61**, 1652–1661.
- Richman DP, Nishi K, Morell SW, Chang JM, Ferns MJ, Wollmann RL, Maselli RA, Schnier J & Agius MA (2011). Acute severe animal model of anti-muscle-specific kinase myasthenia. *Arch Neurol* **69**, 453–460.
- Roche (1935). A case of myasthenia gravis treated at a London County Council Hospital. Video. <http://www.youtube.com/watch?v=uRoRsmvkhTI>. Accessed August 16, 2012.
- Sanders DB, El-Salem K, Massey JM, McConville J & Vincent A (2003). Clinical aspects of MuSK antibody positive seronegative MG. *Neurology* **60**, 1978–1980.

- Sanes JR & Lichtman JW (2001). Induction, assembly, maturation and maintenance of a postsynaptic apparatus. *Nat Rev Neurosci* **2**, 791–805.
- Shigemoto K, Kubo S, Maruyama N, Hato N, Yamada H, Jie C, Kobayashi N, Mominoki K, Abe Y, Ueda N & Matsuda S (2006). Induction of myasthenia by immunization against muscle-specific kinase. *J Clin Invest* **116**, 1016–1024.
- Skeie GO, Apostolski S, Evoli A, Gilhus NE, Illa I, Harms L, Hilton-Jones D, Melms A, Verschuuren J, Horge HW & Societies. EFOF (2010). Guidelines for treatment of autoimmune neuromuscular transmission disorders. *Eur J Neurol* **17**, 893–902.
- Sketelj J, Crne-Finderle N, Sket D, Dettbarn W-D & Brzin M (1993). Comparison between the effects of botulinum toxin-induced paralysis and denervation on molecular forms of acetylcholinesterase in muscles. *J Neurochem* **61**, 501–508.
- Stacy S, Gelb BE, Koop BA, Windle JJ, Wall KA, Krolick KA, Infante AJ & Kraig E (2002). Split tolerance in a novel transgenic model of autoimmune myasthenia gravis. *J Immunol* **169**, 6570–6579.
- Thomsen RH & Wilson DF (1983). Effects of 4-aminopyridine and 3,4-diaminopyridine on transmitter release at the neuromuscular junction. *J Pharmacol Exp Ther* **227**, 260–265.
- Titulaer MJ, Lang B & Verschuuren JJ (2011). Lambert-Eaton myasthenic syndrome: from clinical characteristics to therapeutic strategies. *Lancet Neurol* **10**, 1098–1107.
- Toyka KV, Drachman DB, Griffin DE, Pestronk A, Winkelstein JA, Fishbeck KH & Kao I (1977). Myasthenia gravis. Study of humoral immune mechanisms by passive transfer to mice. *N Engl J Med* **296**, 125–131.
- Viegas S, Jacobson L, Waters P, Cossins J, Jacob S, Leite MI, Webster R & Vincent A (2012). Passive and active immunization models of MuSK-Ab positive myasthenia: Electrophysiological evidence for pre and postsynaptic defects. *Exp Neurol* **234**, 506–512.
- Vincent A, Bowen J, Newsom-Davis J & McConville J (2003). Seronegative generalised myasthenia gravis: clinical features, antibodies, and their targets. *Lancet Neurol* **2**, 99–106.
- Wang X, Wang Q, Engisch KL & Rich MM (2010). Activity-dependent regulation of the binomial parameters p and n at the mouse neuromuscular junction in vivo. *J Neurophysiol* **104**, 2352–2358.
- Wood SJ & Slater CR (1997). The contribution of postsynaptic folds to the safety factor for neuromuscular transmission in rat fast- and slow-twitch muscles. *J Physiol* **500**, 165–176.
- Wu H, Lu Y, Shen C, Patel N, Gan L, Xiong WC & Lei L (2012). Distinct roles of muscle and motoneuron LRP4 in neuromuscular junction formation. *Neuron* **75**, 94–107.
- Wu H, Xiong WC & Mei L (2010). To build a synapse: signaling pathways in neuromuscular junction assembly. *Development* **137**, 1017–1033.
- Wu ZZ, Li DP, Chen SR & Pan HL (2009). Aminopyridines potentiate synaptic and neuromuscular transmission by targeting the voltage-activated calcium channel β subunit. *J Biol Chem* **284**, 36453–36461.
- Xu K, Jha S, Hoch W & Dryer SE (2006). Delayed synapsing muscles are more severely affected in an experimental model of MuSK-induced myasthenia gravis. *Neuroscience* **143**, 655–659.
- Yumoto N, Kim N & Burden SJ (2012). Lrp4 is a retrograde signal for presynaptic differentiation at neuromuscular synapses. *Nature* **489**, 438–442.
- Zhang B, Luo S, Wang Q, Suzuki T, Xiong WC & Mei L (2008). LRP4 serves as a coreceptor of agrin. *Neuron* **60**, 285–297.
- Zhu H, Bhattacharyya BJ, Lin H & Gomez CM (2011). Skeletal muscle IP₃R₁ receptors amplify physiological and pathological synaptic calcium signals. *J Neurosci* **31**, 15269–15283.

Author contributions

M.M., S.W.R., K.V.T. and W.D.P. contributed to the conception and design of the experiments. All of the experiments were performed at Physiology, University of Sydney by M.M. except the quantification of endplate AChE and AChR reorganisation (Figs 8 and 9), which were performed by N.G. (also in Physiology). All authors contributed to the drafting and revision of the article, and approved the final version of the manuscript.

Acknowledgements

We thank the Bosch Institute's Drs Louise Cole (Advanced Microscopy Facility) and Donna Lai (Molecular Biology Facility) as well as Drs Haydn Allbutt, Graham Robertson, Dario Protti and Vladimir Balcar for technical advice. We also thank the apheresis team, Sr Beth Newman, the molecular medicine laboratory at Concord Hospital, Louise Wienholt and patients from around Australia who contributed their plasma to this research. This work was supported by the National Health and Medical Research Council (570930 to W.D.P. and S.W.R.); the Brain Foundation; and Australian Myasthenic Association in New South Wales. K.V.T. was supported by a research grant from the University of Würzburg, Germany.